IEEE Access
Multidisciplinary | Rapid Review | Open Access Journal

Received January 25, 2021, accepted February 6, 2021, date of publication February 12, 2021, date of current version February 24, 2021.

Digital Object Identifier 10.1109/ACCESS.2021.3059233

Bilateral Teleoperation Performance Model for Network Resource Management

KONSTANTINOS ANTONAKOGLOU, (Member, IEEE), MALIHEH MAHLOUJI, AND TOKTAM MAHMOODI, (Senior Member, IEEE)

Centre for Telecommunications Research, Department of Engineering, King's College London, London WC2R 2LS, U.K.

Corresponding author: Konstantinos Antonakoglou (antonakoglou.konstantinos@kcl.ac.uk)

The authors would like to acknowledge the financial support of the Engineering and Physical Science Research Council (EPSRC award reference 1667394).

ABSTRACT In the forthcoming era of the Tactile Internet, haptic communication is foreseen as one of its major use cases with impact in manufacturing, healthcare, education, as well as the service industry. Recent efforts in networking attempt to meet the requirements of such use cases providing the latency and reliability for bilateral teleoperation, the main component of haptic communication. However, the impact of changes in latency on bilateral teleoperation system performance varies among different control schemes and is dependent on the application domain. Furthermore, while recent efforts to reduce latency in wireless communication with tailored configurations have been successful, an increasing number of haptic communication flows could potentially compete when sharing network resources. In this paper, we provide a tractable model for teleoperation system performance that captures the impact of latency on different performance criteria. We then use this performance model to shape queuing prioritisation of different traffic flows. The proposed framework considers the requirements of high and low priority flows to suggest the best possible control scheme option to be used by the high priority one and at the same time keep the impact of the network scheduling discipline on the low priority one at minimum.

INDEX TERMS Bilateral teleoperation, control performance, haptic communication, priority jumps, priority queuing.

I. INTRODUCTION

The upcoming evolution of the Internet, namely the Tactile Internet, will be built upon use case enablers and technologies that can satisfy stringent network requirements. One of the Tactile Internet use cases, haptic communication, will allow improved user immersion to remote environments with the use of multi-modal telecommunication systems [1]. Recent advances in communication networks in enabling fast and highly reliable communication systems can potentially address the requirements of haptic communication [2]. Those include but are not limited to the ultra-reliable low latency communication (URLLC) in the 5th Generation (5G) mobile networks, the ability to run functionalities closer to the user in multi-access edge computing (MEC), and the programmable and finer grain QoS with software-defined networking (SDN).

The associate editor coordinating the review of this manuscript and approving it for publication was Wenchi Cheng.

A major component of haptic communication is bilateral teleoperation, in which a human operator controls a robot with various degrees of freedom in a remote environment and receives feedback from the remote environment. The success of bilateral teleoperation systems depends on accurately replicating the movement of the user (i.e. tracking precision), ensuring and maintaining stability control but also providing high resolution and accurate reaction of the remote environment to the user (i.e. transparency) for a high Quality of Experience (QoE). While bilateral teleoperation is a well-known concept for decades now in various application domains, it heavily relies on stability control methods that compensate for the the lack of performance on communication network between the operator and the operation site [3].

While precision and transparency are important for critical teleoperation applications, such as high precision machinery operation, stability is the essential criterion whose absence diminishes the system's operability. Hence, a wide range of control schemes that guarantee stability have been presented

in the literature, nevertheless, by losing transparency and precision as a trade-off.

In this paper, we devise our attention to traffic prioritisation and specifically prioritisation with priority jumps. The main motivation is to enable highly critical teleoperation applications by reducing their delay, through prioritising their packets in the network. However, simultaneously ensuring that packets belonging to the less critical application but still highly dependent on the network delay, is served in timely manner, through jumps in the queuing. The presented diagram in Figure 1 shows a teleoperation system, where the lower and higher priority queue corresponds to the data packets of the highly critical and less critical teleoperation applications.

Hence, one needs to quantify how delay of the communication network affect performance of the teleoperation system. In order to understand the impact of delay on the performance of teleoperation system, we formulate teleoperation performance, where precision, and transparency are captured as a function of delay. To this end, our contributions are in threefold:

1) A formulation of a polynomial function that captures teleoperation performance in terms of transparency and precision as a function of delay. This model is generic, i.e. can be applied to any control scheme, and has the ability to accommodate future control schemes, with delay dependency. The formulation provides a mapping between order of magnitude of reduction/increase in communication delay and the order of magnitude of improved/degraded control performance respectively, and hence allows for prioritisation of competing flows with the most significant impact on the teleoperation performance.
2) A demonstration of using the formulated polynomial function by employing a dynamic priority scheduling discipline, based on the model of [4], for two different priority flows of highly critical and less critical teleoperation applications.
3) Combining the previous points, we propose a framework which allows comparison of bilateral teleoperation control schemes for different application scenarios as well as optimisation of the dynamic priority queuing system configuration to maximise performance of higher priority haptic communication with minimum effects on the lower priority flow.

The grey boxes in Figure 1 represent the components proposed in this work.

It will be thus possible for teleoperation systems to incorporate multiple control schemes and switch between them for achieving the best performance with minimum cost to the communication platform.

The structure of the paper is as follows. In Section II we present relevant indicative works on the topic of management of Tactile Internet enablers with respect to meeting use case QoS requirements and QoE performance. Section III

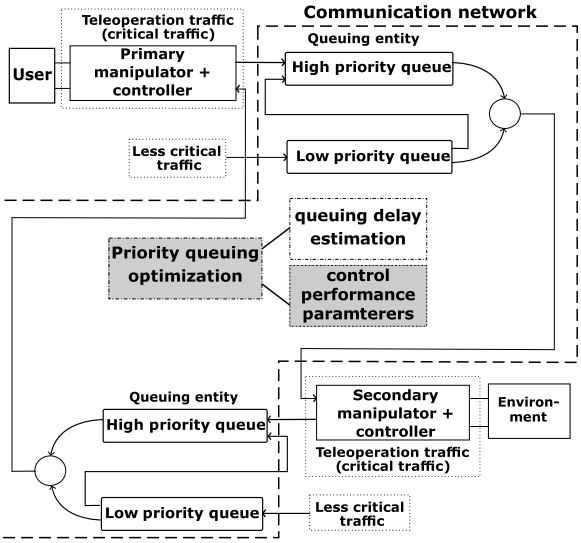

FIGURE 1. System diagram with a communication network accommodating high and low priority critical flows.

first discusses the teleoperation system control performance, followed by an analysis and results of the proposed control performance model. Section IV presents an overview of dynamic queuing mechanisms and an analysis of the queuing mechanism used within the proposed framework. Section V includes a discussion on the framework's capabilities for selecting an appropriate teleoperation control method to satisfy delay requirements of prioritised traffic. Section VI presents the formulation, description and discussion of results of a bi-objective optimisation problem our framework targets to solve. We conclude this paper in section VII.

Finally, for the sake of readability and due to the multidisciplinary nature of this work, acronyms and mathematical symbols have been summarised in the Appendix.

II. BACKGROUND

This section discusses works that focus on monitoring QoE for use cases such as bilateral teleoperation in order to manage Tactile Internet enablers to meet the requirements of URLLC applications.

It must be noted that only a few methodologies and frameworks consider the capabilities of bilateral teleoperation to compensate for the delays induced within the different network domains. Such efforts focus on making the network more application-aware with respect to system and QoE performance. In [5], the authors present a framework that incorporates a supervised deep learning methodology that incorporates both objective and subjective performance criteria. In [6], a QoE model based on user feedback is used for fog computing resource management. These efforts are used for measuring QoE of a wide range of Tactile Internet use cases.

Focusing more on bilateral teleoperation, the authors of [7] propose the use of impedance error combined with human perception resolution as a measure of QoE for traffic

management within NFV infrastructure, but without taking into account further use of methods to maintain stability of the system under large communication delays.

An approach for modelling a QoE performance function based on experimental results is described in [8] which involves subjective ratings of the performance of control schemes of time-domain passivity and model-mediated teleoperation approaches.

In this regard, radio resource allocation to improve QoE of the users is proposed in [9] by analysing traffic traces of teleoperation data traffic as well as in [10] by considering a delay-based QoE model for two cases of bilateral teleoperation frameworks.

Additionally, during their operation, networks serve a variable amount of data traffic. In many cases, during certain time periods, traffic congestion needs to be managed to reduce its latency-inducing effects and provide the required QoS to traffic flows. In [11], the authors present a method that multiplexes bilateral teleoperation traffic and sensor traffic of lower priority modelled as deterministic and stochastic traffic respectively. In this approach latency overprovision of high priority traffic is averted by allowing high priority traffic frames to be overwritten by low priority traffic frames assuming a certain reliability threshold is not exceeded. Nevertheless this approach is valid only for certain scenarios.

Finally, the aforementioned efforts have contributed in QoS provision for URLLC traffic, nevertheless, in a survey on Time-Sensitive Networks (TSN) and Deterministic Networking standards [12], it is stated that future efforts need to focus towards the direction of dynamically managing flow prioritization.

III. MODELLING CONTROL PERFORMANCE

A. CONTROL PERFORMANCE AND STABILITY OF TELEOPERATION

Plethora of control schemes have been presented in the literature for teleoperation systems, each with its advantages and disadvantages [3]. Choosing the most appropriate control scheme is only possible through understanding of the properties of communication network, e.g. whether delay is constant or variable, bounded or unbounded, information available from the remote environment, e.g. whether the model of the remote environment is available, the environment structure, desired performance, and implementation aspects of the application.

The main components of a teleoperation system are illustrated in Figure 1 within the scope of the proposed system design. In this diagram, the operator, the environment, and primary and secondary manipulators remain the same for all control schemes, while primary controller and secondary controller are implemented differently depending on the control scheme.

The aim of this section is to elaborate on how the above dependencies could be captured in a generic performance model of the teleoperation system. Our focus here is to capture mainly the effect of communication delay on the control performance. Such model will allow us to choose the most appropriate control scheme given the characteristics and value of the communication delay or to configure the communication network in order to support a chosen control scheme. Ultimately, we can analyse successful delivery of the teleoperation system over a communication network, where a range of configurations are available for both the teleoperation control scheme and the communication network.

To this end, we review *stability* criteria, and performance of a set of control schemes in this section. The performance is described in terms of *transparency* and *tracking precision* which will be further analysed with regard to their sensitivity to the order of magnitude of delay (i.e. whether performance is affected by delay linearly, exponentially, etc.), as well as dependency on knowing the exact value of delay, and having knowledge of the remote environment dynamics.

The most important criterion for any controller is stability, the main goal of any control scheme, which, in teleoperation, is highly dependent on the communication delay [13]. A stable system can be either *intrinsically stable* (IS), i.e. stable for all values of communication delay (d) and control parameters, or *possibly stable* (PS), i.e. stable for all delay values under specific control parameters and stable for delay values less than a maximum value, for other control parameters [14].

Performance of control schemes in terms of *transparency* and *tracking precision* can be captured through the following metrics [14]:

- *Inertia (M_p) and damping (B_p)* perceived by the primary when no force is applied to the secondary manipulator by the environment; M_p and B_p affect transparency.
- *Tracking error (δ)* of the primary manipulator position versus the secondary manipulator when no force is applied by the environment to the secondary manipulator; δ affects tracking precision.
- *Stiffness (K_p)* perceived by the primary when force is exerted to the secondary manipulator by the environment; K_p also affects transparency.
- *Position Drift (Δ)* when a force is exerted to the secondary manipulator by the environment, which impacts tracking precision.

As mentioned above, the first three metrics (M_p, B_p and δ) can be considered during movement without interaction with the remote environment, whereas the latter two parameters (K_p and Δ) play a role only when there is interaction with the remote environment.

The M_p, B_p, and K_p affect the transparency of the teleoperation system; in other words the quality of telepresence of the operator (primary) at the remote (secondary) side. For perfect telepresence, M_p, and B_p should be equal to the remote environment's inertia and damping (assuming no external environmental force), and K_p should be the same as the environment stiffness. On the other hand, δ and Δ, affect the tracking precision and represent precision of the teleoperation

system. For a high precision teleoperation system, tracking error δ and position drift Δ should be negligible [15].

The two equations governing the teleoperation system, as depicted in Figure 1, are described in Eq. 1 and based on the work in [14]:

$$F_m = F_h - F_{mc}, \quad F_s = F_e + F_{sc}. \tag{1}$$

In Eq. (1), F_h and F_e refer to the human (operator) force and the environment force imposed on the primary and secondary manipulator, respectively. The F_{pc} and F_{sc} are the forces of primary and secondary controller which are computed based on the control schemes. Therefore, F_m and F_s are the resulting forces applied on the primary and secondary manipulators respectively.

For the analysis in this paper, similar to [14], we assume that primary and secondary manipulators have identical mass-damper dynamics as follows:

$$F_m = M_m s^2 x_m + B_m s v_m, \quad F_s = M_s s^2 x_s + B_s s v_s, \tag{2}$$

where x_m, x_s, v_m, v_s are the positions and velocities of the primary and secondary manipulator respectively, s is Laplace transform variable, M_m, B_m, M_s and B_s are mass and viscous coefficients of primary and secondary manipulator respectively. Given the identical assumption above, $M_m = M_s$ and $B_m = B_s$. In the case of force exertion from the environment on the secondary manipulator, the environment is modelled as a spring-damper, as described in Eq. (3).

$$F_e = -(B_e + \frac{K_e}{s})v_s, \tag{3}$$

An ideal bilateral teleoperation system would satisfy the following,

$$M_m - M_p = 0,\ B_m - B_p = 0,\ K_e - K_p = 0,\ \delta = 0,\ \Delta = 0 \tag{4}$$

Of course, in reality teleoperation systems do not operate under ideal conditions and therefore the differential values in (4) are always non-zero in the presence of delay.

The control schemes of interest in this paper are Force Reflection (FR), Predictive Control (PC), Position Error (PE), Adaptive Motion/Force Control (AMFC) and Predictive Controller with Passivity (PCP). More specifically for PC the Smith predictor is used, while PCP uses a combination of the wave variables approach and the Smith predictor.

The above are indicative control schemes, either PS or IS as well as from different classes of teleoperation control techniques such as passivity-based control, predictive control and model-free control, which can be considered during the teleoperation system design phase based on the goals and scenarios that it will be used in, to maintain stability and achieve acceptable transparency. A summary of delay-dependency of the aforementioned control schemes' performance can be found in Table 1, including their stability category (i.e. PS or IS) and the need for prior knowledge of delay. Further discussion and details for the above schemes can be found in [14].

B. MODELLING CONTROL PERFORMANCE WITH RESPECT TO COMMUNICATION DELAY

In this section, we describe how control performance can be modelled as a function of communication latency. After reviewing the different control schemes presented in Section III-A and their respective performance metrics, we express control performance as a loss function. The *Control Performance Loss Function* (CPLF) reveals the loss in perceived inertia (M_p) versus the manipulator's inertia (M_m), perceived damping (B_p) versus the manipulator's damping (B_m), perceived stiffness (K_p) versus environment stiffness (k_e), tracking error (δ) and position drift (Δ). As shown in Equation (4), the best performance of teleoperation system is achieved when $M_m = M_p$, $B_m = B_p$, $k_e = k_p$, $\delta = 0$, and $\Delta = 0$. In this equation, weight values w_i are used to normalise the contribution of the different loss values depending on the teleoperation scenario. For example, a teleoperation system used in underwater inspection will be more tolerant in movement accuracy than a system used for MIS, therefore in the MIS case the contribution of the movement accuracy loss values should be greater and therefore the corresponding weights should be increased.

$$CPLF = w_1(\frac{M_m - M_p}{M_m})^2 + w_2(\frac{B_m - B_p}{B_m})^2 + w_3(\frac{K_e - K_p}{K_e})^2 + w_4\delta^2 + w_5\Delta^2. \tag{5}$$

Due to the possible high orders of magnitude of inertia, damping and stiffness compared to tracking and drift error values and to ease the selection of weights w_1, w_2 and w_3 respectively, it can be noticed that we normalise these parameters. To further clarify Eq. (5), we elaborate the loss function for one of the control schemes, explained earlier in Section III-A. In the PCP control scheme, the control parameters of inertia, damping, stiffness, tracking error, and drift error can be expressed as follows [14],

$$\text{Perceived inertia } (M_p): \quad 2M_m - \frac{B_m^2}{K_c} \tag{6}$$

$$\text{Perceived damping } (B_p): \quad 2B_m \tag{7}$$

$$\text{Tracking error } (\delta): \quad \frac{B_m + K_c d}{2B_m K_c} \tag{8}$$

$$\text{Stiffness } (K_p): \quad \frac{K_e K_c (B_i + B_m)}{(K_e + K_c)(B_i + B_m) + 2K_e K_c d} \tag{9}$$

$$\text{Drift error } (\Delta): \quad \frac{B_i + B_m + 2K_c d}{(B_i + B_m)K_c} \tag{10}$$

where B_i is the impedance of the communication network, K_c a control parameter and d is the one-way delay of the communication network. It can be seen that while the two primary parameters are delay-independent, the latter three parameters have dependency to d, d^{-1}, and d respectively. In order to capture the relationship between the loss function, CPLF, and the communication delay in a generic form, we formulate a

polynomial function:

$$CPLF(d) = \sum_{l} \phi_l d^l, \quad l \in \{-1, 0, 1, 2\}. \tag{11}$$

This formula is based on Eq. (5) and substitution of the corresponding control parameters of the chosen control scheme. The coefficients ϕ are the result of algebraic work according to Eq.5. The polynomial degrees are considered to be between -1 and 2 based on the observations from control schemes under discussion. Table 1 allows a comparison of the chosen control schemes in terms of their stability category (PS or IS), if prior knowledge of delay d is required for the schemes to operate, and how their performance metrics are dependent to delay d. Clearly $l = 0$ capture the effect of those loss values that are not delay dependant.

TABLE 1. Comparison of control schemes with respect to delay.

Scheme	Stability	Known d	M_p	B_p	K_p	δ	Δ
FR	PS	No	$\propto d$	-	-	$\propto d$	-
PC	PS	No	-	-	-	$\propto d$	-
PE	PS	No	$\propto d, d^2$	$\propto d$	-	-	-
AMFC	PS	No	$\propto d$	$\propto d$	-	-	-
PCP	IS	Yes	-	-	$\propto 1/d$	$\propto d$	$\propto d$

In the next sections, we first present a methodology through which we can select the most appropriate control scheme to be used under certain communication network conditions and given teleoperation application domain. Finally, an optimisation problem is formulated for delivering maximum control performance with minimum impact on the resource utilisation.

IV. PRIORITY QUEUING MODEL

A. PRIORITY QUEUING WITH PRIORITY JUMPS

In this section, we focus on the aspect of network scheduling and specifically traffic prioritisation in queuing systems, in order to serve multiple classes of high priority traffic but with different order of importance. A well-known and widely implemented traffic prioritisation discipline is Strict Priority (SP) queuing. The SP has been proposed for service differentiation in the Internet [16], but with a major shortcoming. In SP, packets of low-priority queues are served only if higher priority queues are empty, which results in starvation of low-priority traffic.

To reduce the effects of starvation, dynamic priority scheduling has been studied in the literature [17]. One of the strategies to minimize starvation is Head-of-Line Priority Jump (HOL-PJ) first presented in [18] where the priority of packets entering the system is altered during execution of the queuing system, instead of using absolute priorities. Effectively, this results in a parameterized moderation of system performance with a focus on fairness among different classes of traffic being served by the system. Many implementations use the concept of priority jumps (also known as priority upgrades) by changing priority levels of each packet waiting in one or more queues depending on the system model.

For the rest of Section IV-A, we present indicative works on the topic of dynamic priority scheduling non-preemptive disciplines including the discipline that is used in our proposed framework in this paper. We will omit disciplines that use time-stamping for changing packet priority, a process which increases computation requirements.

Even though many performance indicators can be used for dynamically changing service of prioritised traffic, probabilistic disciplines offer more flexibility as the parameterization can also be user-controlled, allowing the system designer to select the criterion or criteria that will affect performance of the queues using the same queuing discipline. In [19], the queue-based Probability Priority (PP) discipline is proposed. In PP system model, based on the p_i-persistent protocol, every queue is assigned a user-selected probability which affects the choice of the next queue to be served, also known as probabilistic service. The Head-Of-Line Merge-By-Probability (HOL-MBP) scheduling discipline, lies within the packet-based category of disciplines. For simplicity, assuming a single-server system of two priority queues (one for high and one for low priority traffic), packets of low priority traffic queue to the high priority queue according to a user-defined probability [4].

In this paper, the model presented in [4] is being used as one of the two main components of the proposed framework. The model is useful because of its user-controlled parameterization property which is desirable for our framework, as explained further in Section IV-B. Nevertheless, it should be highlighted that the control performance model presented in Section III-A is not limited to be integrated only with the specific queuing discipline but with any other system that would benefit from prior knowledge of bilateral teleoperation performance under different values of delay.

B. DELAY ANALYSIS OF PRIORITY QUEUE WITH JUMPS

As discussed earlier, probabilistic prioritisation queuing disciplines offer flexibility in terms of selecting which criteria to influence the behaviour of the queuing system. Furthermore, because of the characteristics of bilateral teleoperation traffic, i.e. small payload and high rate of packet generation, the prioritisation model should allow simple per-flow distribution of different priority queues, with fine granularity characteristics, affecting traffic in a per-packet basis. Hence, we choose to use the HOL-MBP model, due to above mentioned properties as well as tractability of analysis based on probability generating functions (PGFs). For the rest of this section we will present the analysis of such a queuing model.

The system model, as seen in Fig. 1, shows two level of priority for traffic, the high priority (class 1), corresponding to critical traffic, and one low priority (class 2), corresponding to less critical traffic, each directed to First Come First Serve (FCFS) queues. For the analysis of the system we assume that time is slotted and one slot n is equal to the transmission time of one packet. The arrival processes for both types of packets with arrival rates λ_1,λ_2 are modelled as Poisson processes. Furthermore, queues are of infinite

capacity, the system is work-conserving (i.e. it is never idle) and the service time of each packet is equal to one time slot.

Though with the SP discipline, the low priority queue would be served only when high priority queue is empty, in HOL-MBP, during time slot n, packets from low priority queue (all waiting packets plus those which arrive during slot n) may jump to the high priority queue with a probability of β. This jump can occur both when high priority is empty or non-empty. The equations that describe how the content of each queue evolves in time are shown in [4] (Section 3, equations [1]-[4]).

The equations of interest to this paper, among those discussed in [4] are:

- the total number of packets in the system:

$$E[p_T] = \lambda_T + \frac{\lambda_{TT}}{2(1-\lambda_T)} \tag{12}$$

- the mean value of waiting time in high priority queue:

$$E[d_H] = 1 + \lambda_2 - \frac{1-\lambda_1}{\beta} + \frac{\lambda_{TT}\lambda_1 + \lambda_{11} - \lambda_{11}\lambda_T}{2(1-\lambda_T)\lambda_1} \tag{13}$$

$$- \frac{(1-\lambda_T)A_T(Y(\beta,1))}{Y(\beta,1) - A_T(Y(\beta,1))} \tag{14}$$

- the mean value of delay of any arbitrary packet:

$$E[d] = \frac{\lambda_1}{\lambda_T}E[d_H] + \frac{\lambda_2}{\lambda_T}E[d_L] \tag{15}$$

where, λ_T is the total arrival rate ($\lambda_T = \lambda_1 + \lambda_2$), λ_{11} and λ_{TT} the second partial derivatives of the PGF of the joint arrival process, A_T the PGF of the total number of arrivals and Y a factor which can be obtained numerically (in our case we used the bisection approximation method with initial values 0 and 1).

Since directly calculating the mean value of waiting time in low priority queue is complex, and it has been proven that $E[p_T] = \lambda_T E[d]$ [4], combining three equations of (12)-(15), one can calculate $E[d_L]$, as follows,

$$E[d_L] = \frac{\lambda_T}{\lambda_2}(\lambda_T E[p_T] - \frac{\lambda_1}{\lambda_T}E[d_H]) \tag{16}$$

Eq. (14) and (16) show that both low and high priority delay values, i.e. d_H and d_L, depend on the parameter β. Our optimization framework will, hence, define parameter β to meet the minimum requirements of low priority traffic.

V. CHOICE OF CONTROL SCHEME

A. CONTROL SCHEME SELECTION

By combining the previously mentioned network scheduler and proposed control performance model of Sections IV-B and III-B respectively, this section presents a methodology with which the proposed combination can satisfy the requirements of both high and low priority critical traffic flows while focusing on providing good quality of telepresence to the user. This methodology concerns the selection of the most suitable control scheme assuming prior knowledge of the delay requirements of low priority critical flow delay.

An advantage of calculating CPLF of a set of available control schemes for different delay values is the ability to quantitatively compare these control schemes among each other. In this way, it is possible to choose which one is more suitable for the purpose of the desired bilateral teleoperation application scenario. Further reduction of the available options is possible considering that some control schemes may not be acceptable for use given a certain application scenario, e.g. ability of the control scheme to maintain stability of the system in the presence of delay caused by long distance communication.

To easily demonstrate the aforementioned comparison, we observe the behaviour of control schemes' CPLF for a fixed value of β. Later in this paper, an optimization framework will be presented for optimizing the choice of β for control schemes individually.

To begin with, it is necessary to calculate the possible queuing delays for both flows for $\beta \in [0, 1]$. Assuming prior knowledge of low queuing delay value t_L that meets the requirements for low priority critical traffic, it is possible to find the high priority critical traffic flow queuing delay as t_L will correspond to a certain β value. Therefore, it is possible calculate CPLF for all desired control schemes. Once CPLF values are determined by also taking into account the teleoperation scenario, it is possible to select the most suitable control scheme.

Of course, for the computation of CPLF, as shown in Section III, several teleoperation and control scheme configuration parameters need to be initialized. For possibly stable control schemes these parameters determine the delay that can be tolerated in order for the system to remain stable. These stability thresholds can further narrow down the selection of the most suitable control scheme.

B. SIMULATION

In this section we present performance evaluation of the control scheme selection framework, for a diverse set of scenarios, selected to represent different teleoperation application classes. The simulation focuses solely on the impact of latency on the proposed system. This work neither investigates the impact of jitter, which is usually managed by employing buffers (therefore increasing end-to-end latency), nor packet loss which has little impact compared to the previous QoS metrics. Furthermore, the simulation setup, the assumptions and values used are explained in Section V-B1 and afterwards the numerical results are presented in Section V-B2.

1) SIMULATION SETUP

We setup two simulation models in Matlab, one for the dynamic priority network scheduler as presented in Section IV-B and one for CPLF of each control scheme for different weight values as shown by Eq. (5).

For the queuing system simulation, we assume the available transmission rate for both critical flows is 5 Mbps and packets are all of equal size of 255 Bytes. Packet size is

TABLE 2. Simulation values.

Communication parameter		Value
Packet size		255B
Available transmission rate		5 Mbps
Total link utilization λ_T		0.95
Traffic balance α		0.5
Teleoperation parameter		**Value**
Mass $M_m\,(kg)$		10
Damping $B_m\,(kg/s)$		1
Stiffness $K_e\,(N/m)$		10
Gain G_c		1
Control Scheme	**Parameter**	**Value**
FR (Configuration 1)	Gain K_c	10
FR (Configuration 2)	" K_c	100
PE (Configuration 1)	" K_c	10
PE (Configuration 2)	" K_c	100
PC	" K_c	100
PCP	" K_c	100
	Impedance B_i	1
AMFC	A	0.006
	C	50
	Gain K_m	$10 \cdot M_m$
	Λ	1

chosen based on work presented in 3GPP Technical Specification 23.501 [20] for motion control traffic. Additionally, similar to IV-B, one time slot is equal to the transmission time of a packet. Hence, calculating transmission time knowing the size and transmission rate is intuitive. We further assume a stable queuing system, with traffic rate λ_T that corresponds to 95% utilisation of the server and that arrival traffic balance $\alpha = \frac{\lambda_1}{\lambda_T} = 0.5$. For the purpose of demonstrating the control scheme selection for a given low priority flow delay requirement, delay value d_L, is set to 10 ms.

With regard to the CPLF simulation, CPLF equations for different control schemes are implemented with teleoperation parameters as detailed in Table 2. Specifically for control schemes FR and PE, two different configurations of parameters, affecting control performance as well as their delay tolerance, are used. It is important to note that only performance in the stable region of each control scheme is examined. Additionally, the implemented control scheme PCP is intrinsically stable, hence there is no delay threshold. The delay threshold for the possibly stable PC is 120 ms whereas AMFC is tolerant to any delay for certain parameter values as explained in [14]. Finally, we assume parameters of the remote environment are constant during the simulation, therefore delay thresholds will remain the same throughout the simulation. This also allows this work to focus on the variations of the communication network.

2) SIMULATION RESULTS

We first look into the values of d_L and d_H and how they are affected by changing of β. Fig. 2 shows the two values of d_L, and d_H, versus β. It could, for example, be seen that at the low priority delay value of $d_L = 10$ ms, corresponds to a beta value $\beta = 0.18$ and $d_H = 7$ ms, as illustrated by the dotted lines of Fig. 2.

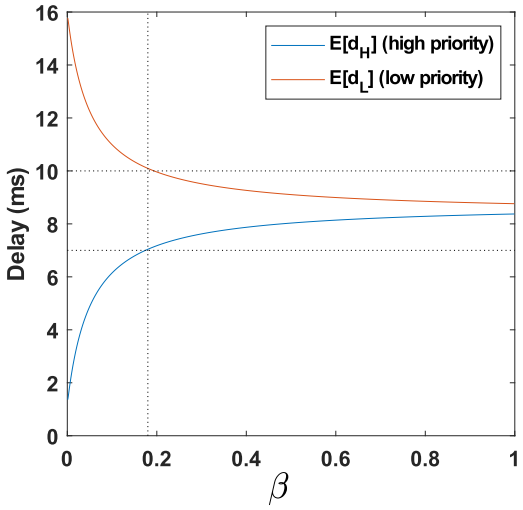

FIGURE 2. Mean value of packet delays versus beta.

The plots of Fig. 3 and Fig. 4 present the calculated and normalized CPLF values of each control scheme for time delay $d \in [0, 0.13]$ in seconds. Nevertheless, according to the results of Fig. 2, the delay value range of interest, i.e., the values of d_H, for all plots of Fig. 3 and Fig. 4 is 1.4 to 8.4 ms. Additionally, each row concerns the two different possible configurations for FR and PE control schemes and each column corresponds to a different teleoperation application case.

At this point, it is important to note that CPLF values as presented in Fig. 3 and Fig. 4 have been normalized based on the percentage of decrease of a control scheme's CPLF compared to CPLF of FR scheme hence FR CPLF is not directly shown in the plots:

$$CPLF(i)_{norm} = \frac{CPLF(FR) - CPLF(i)}{CPLF(FR)} \cdot 100, \qquad (17)$$

where i $\in$ {PE, PC, AMFC, PCP} as described in III-A. Higher decrease of CPLF of a control scheme compared to FR means improved performance. In each plot, line β (corresponding to $d_H = 7$ ms) indicates the high priority queuing delay (x-axis) point at which the comparison takes place. A positive percentage (y-axis) means better performance than FR, i.e. CPLF of FR has a higher value than the control scheme in question, while a negative percentage means that FR performs better. In this way, control schemes can also be compared among each other. The last step is the selection of the control scheme that performs best according to the communication network delay set previously (which in turn affects the position of line β).

Based on the aforementioned numbers and assumptions we demonstrate the control scheme selection for two different configurations of control parameters of FR and PE control schemes, Configurations 1 and 2 in Fig. 3 and Fig. 4 respectively (as shown in Table 2). We also present results for four different cases of CPLF weights corresponding to four different teleoperation scenarios:

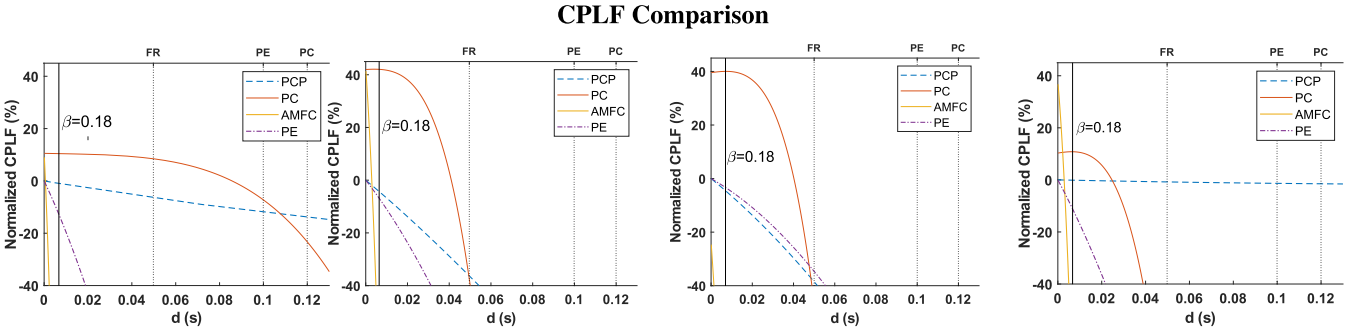

(a) Scenario 1: Lower sensitivity to tracking error

(b) Scenario 2: Higher sensitivity to tracking and drift error

(c) Scenario 3: Higher sensitivity to tracking and drift error and lower sensitivity to inertia, damping and stiffness

(d) Scenario 4: Higher sensitivity to inertia, damping and tracking error

FIGURE 3. Comparison of CPLF among different control schemes in four different scenarios (i.e. different weight choices) for Configuration 1 of FR and PE control scheme parameters.

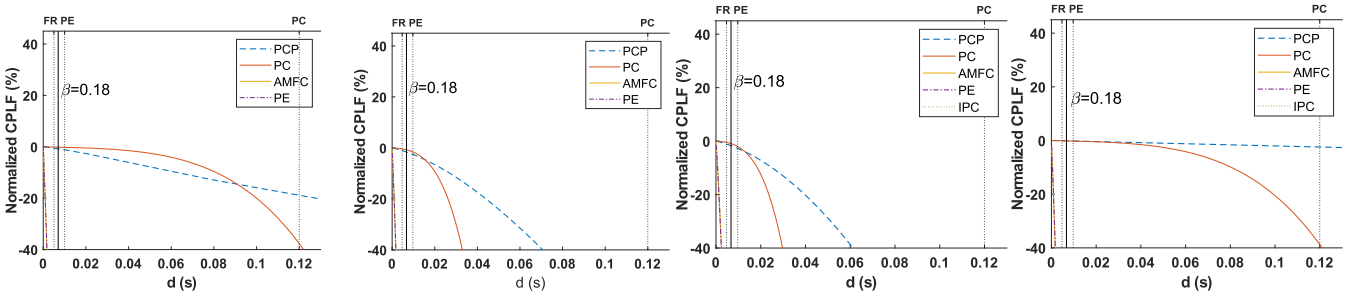

(a) Scenario 1: Lower sensitivity to tracking error

(b) Scenario 2: Higher sensitivity to tracking and drift error

(c) Scenario 3: Higher sensitivity to tracking and drift error and lower sensitivity to inertia, damping and stiffness

(d) Scenario 4: Higher sensitivity to inertia, damping and tracking error

FIGURE 4. Comparison of CPLF among different control schemes in four different scenarios (i.e. different weight choices) for Configuration 2 of FR and PE control scheme parameters.

- *Scenario 1*: Equal participation of all performance metrics with weights $w_1, w_2, w_3, w_4, w_5 = 1$. This case refers to applications where tracking capabilities are not as important such as bilateral teleoperation for underwater inspection or other systems with semi-autonomous capabilities.
- *Scenario 2*: Increased participation of tracking and drift error by choosing weights $w_1, w_2, w_3 = 1$ and $w_4, w_5 = 100$, can be relevant to applications such as minimal invasive surgery.
- *Scenario 3*: Increased participation of tracking and drift error with reduced participation of inertia, damping and stiffness in the calculation of CPLF by choosing weights $w_1, w_2, w_3 = 0.5$ and $w_4, w_5 = 100$. Possible applications can be certain cases of micro-assembly, e.g. rotational movements.
- *Scenario 4*: Participation of inertia, damping and tracking only with weights $w_1, w_2 = 1$, $w_4 = 100$ and $w_3, w_5 = 0$. This choice of weights corresponds only to free-space movement applications.

It must be noted that the case of participation of performance metrics with weights $w_1, w_2, w_3 > 1$ and $w_4, w_5 \leq 1$, meaning increased participation of inertia, damping and stiffness but decreased participation of tracking and drift error, provides virtually the same results as in Scenario 1.

As previously discussed, $d_L = 10$ ms is an acceptable low priority traffic latency which corresponds to $\beta = 0.18$. This β value is used to calculate d_H using Equation (14) and therefore it is possible to compare CPLF values of control schemes for this specific delay, for the four application scenarios.

Regarding the results presented, we can first discuss the behaviour of the plots of Configuration 1 in Figure 3 compared to those of Configuration 2 in Figure 4. As a reminder, the difference between these groups of plots lies in the recalculation of CPLF, due to changing control parameter K_c for control schemes PE and FR. The latter control scheme is also used for normalising the CPLF values of all other control schemes as shown in 17. Furthermore, due to the increased value of control parameter K_c, from $K_c = 10$ in Configuration 1 to $K_c = 100$ in Configuration 2, there is an increase increase of performance in FR therefore lower values of normalised CPLF can be observed in Configuration 2 than in Configuration 1. Nevertheless, due to the trade-off of stability and transparency, this performance increase comes with a cost of a reduced stability threshold, which, as illustrated by the dotted line for FR, is 5 ms in Configuration 2 from 50 ms

in Configuration 1. Similarly, the stability threshold for PE also decreases by increasing K_c, from 100 ms to 10 ms.

Focusing more on the comparison among the control schemes illustrated by lines of different colour, we take into account the vertical β line, which is drawn to indicate the latency value under which the critical traffic flow operates. We use the β line to see which control scheme has the highest CPLF value and if this value is positive.

It can be observed that for all scenarios of Configuration 1, PC is the best possible choice for the selected β value. In Configuration 2, PC is the best choice in all scenarios with the exception of scenario 4 where PCP and PC are equally good choices. In more detail for Fig. 4(b) and 4(c), even though the normalised CPLF values for PC in are negative, the FR control scheme stability threshold is lower than the delay imposed by the selected β value and therefore FR cannot be considered as an option.

In some cases such as Fig. 3(a) and 3(d), it can be seen that for lower values of high priority delay (and therefore lower β) control scheme choice becomes more competitive, nevertheless, it needs to be noted that in bilateral teleoperation the choice of the control scheme is an important system design decision that is affected by several factors. These factors can include (but not limited to) the type of interaction that the haptic system enables the user to have with the remote environment (e.g. direct or model-mediated), the number of degrees of freedom and the operational input signal frequency range which will affect the stability region of the system. As a result, these factors may affect the behaviour of the CPLF of the control schemes but may also have to be taken into account when selecting the best control scheme.

VI. OPTIMISATION OF PRIORITY QUEUE PERFORMANCE

In this section, we present a bi-objective optimization problem that maximises control performance of the system for a high priority teleoperation traffic, i.e., critical URLLC, while minimising communication delay for the lower priority non-critical URLLC traffic.

The first objective (problem P_1) of the optimisation problem is to maximise control performance, i.e., to minimise CPLF. The control performance function of CPLF represents the loss in transparency and movement precision as a result of delay $E[d_H]$ on communication between primary and secondary controller.

The second objective (problem P_2) is the minimisation of delay $E[d_L]$ for the non-critical URLLC traffic. Both of these delays change values as a function of *beta* and therefore the corresponding objective functions can be modelled as functions of β. Our goal is to find to balance between delay incurred to the non-critical traffic and the performance of critical teleoperation traffic.

After the selection of a control scheme and since the delay of the critical URLLC traffic is $E[d_L]$, the objective function for problem P_1 can be formulated by using the corresponding CPLF equation replacing d with $E[d_H]$. Therefore, based on the polynomial in Equation (11) P1 can be formulated as:

$$P_1(\beta) = CPLF(\beta) = \sum_l \phi_l E[d_H]^l, \quad l \in \{-1, 0, 1, 2\}, \tag{18}$$

with $E[d_H]$ as defined in Equation (14).

The objective function for Problem P_2, which concerns the minimisation of $E[d_L]$ that is defined as in Equation (16), can be formulated by also expanding $E[d_H]$ using Equation (14):

$$\begin{aligned} P_2(\beta) &= \frac{\lambda_T}{\lambda_2}(\lambda_T E[p_T] - \frac{\lambda_1}{\lambda_T} E[d_H]) \\ &= \frac{\lambda_T}{\lambda_2}\left(\lambda_T E[p_T] - \frac{\lambda_1}{\lambda_T} - 1 + \lambda_2 - \frac{1-\lambda_1}{\beta}\right. \\ &\quad \left. + \frac{\lambda_{TT}\lambda_1 + \lambda_{11} - \lambda_{11}\lambda_T}{2(1-\lambda_T)\lambda_1} - \frac{(1-\lambda_T)A_T(Y(\beta,1))}{Y(\beta,1) - A_T(Y(\beta,1))}\right). \end{aligned} \tag{19}$$

Using P_1 and P_2 we can find the right balance between delay incurred to the low priority traffic and the performance of high priority teleoperation traffic. To this end, we formulate a problem that configures the value of *beta* for maximising teleoperation performance, i.e., lowest value of loss as captured in $CPLF(d)$ in Equation (18), while also ensuring the lower priority traffic achieves the lowest possible latency, as captured in Equation (19). The method used to formulate the problem is the Weighted Sum Scalarisation method (as in Equation (3) in [21]). Therefore, the optimisation problem can be formulated as:

$$\begin{aligned} &\underset{\beta}{\text{minimise}}\ F(\beta) = \gamma_1 \frac{P_1(\beta)}{sf_{1,0}(\beta)} + \gamma_2 \frac{P_2(\beta)}{sf_{2,0}(\beta)} \\ &\text{subject to } 0 < \beta < 1, \end{aligned} \tag{20}$$

where $F(\beta)$ is the master problem objective function and $sf_{1,0}(\beta)$ and $sf_{2,0}(\beta)$ are normalisation factors for transforming the objective functions so that they have similar orders of magnitude and adapt units, so that they are both comparable. Another important aspect of this formulation are the scaling parameters that have a sum of 1, therefore by choosing γ_1 for P_1 we get $1 - \gamma_1 = \gamma_2$ for P_2. Nevertheless, the objective function of Equation (20) can be reformulated without normalisation and in this case the weights chosen can have a sum different than 1. The use of weights is significant for revealing the relative importance between P_1 and P_2.

The proposed problem can be expanded by adding an additional constraint on beta. Due to the stability thresholds of each control scheme, as presented in the previous section, in certain cases where the stability threshold is within the range of delay values of $E[d_H]$, an change of the value of beta should not allow the $E[d_H]$ value to exceed the threshold. Nevertheless, such a case is not studied in the formulation of this problem. Excluding the case of considering a stability threshold, it can be observed that all possible values of $P_1(\beta)$ and their corresponding values $P_2(\beta)$ for the same β, are also all the possible solutions of the master problem $F(\beta)$. Therefore, for this problem there are no dominated solutions.

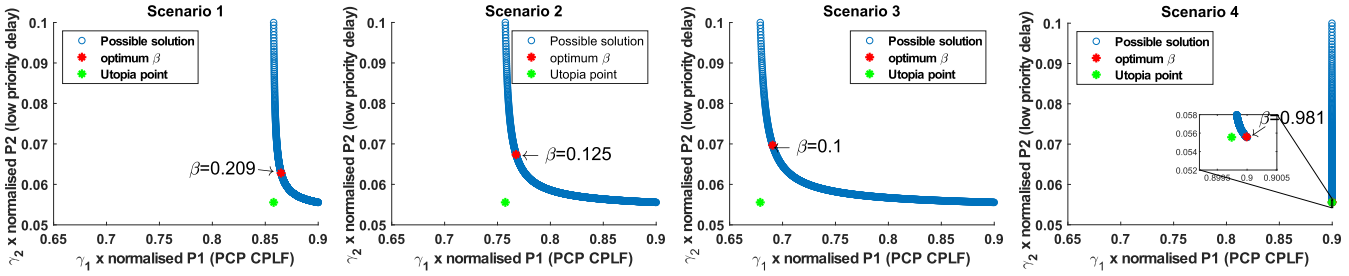

(a) $\gamma_1 = 0.1$ and $\gamma_2 = 0.9$

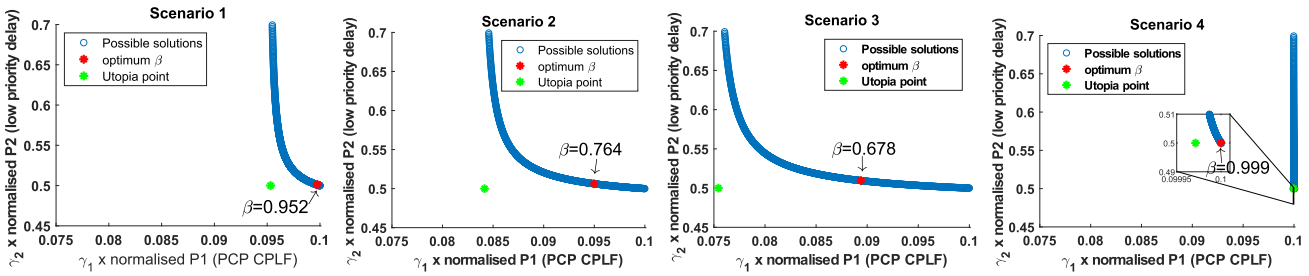

(b) $\gamma_1 = 0.9$ and $\gamma_2 = 0.1$

FIGURE 5. Optimisation of β for four different application scenarios and scaling parameter values γ_1 and γ_2.

The optimisation problem as formulated in Equation (20) using the Weighted Sum method is reduced from a bi-objective problem to a single objective problem solved using the principle of Pareto optimality or else Pareto efficiency [22].

A. NUMERICAL RESULTS

In this subsection, we present numerical solutions and their interpretations for the optimization problem formulated in the previous section. Figure 5, presents two sets of plots of possible P_1 solutions against possible P_2 solutions, based on the simulation parameter values for CPLF and the priority queuing model set in Section V.

Moreover, the solutions of both objectives of the optimisation problem presented in this section concern PCP control scheme in the four different teleoperation scenarios enlisted in Section V-B2 as well as for two different values for the scaling parameters γ_1 and γ_2 of Equation (20). For the normalisation factors $sf_{1,0}$ and $sf_{2,0}$, we use the maximum values of P_1 and P_2 respectively.

Both sets of plots in Figures 5(a) and 5(b), display the Pareto front of solutions for P_1 and P_2. The solutions in the criterion space of the optimisation problem are the calculated values of CPLF that correspond to the values of $E[d_L]$ for $\beta \in [0, 1]$. These values are all possible non-dominated solutions (in blue). For each of these plots, the optimal solution is the one with the minimum Euclidean distance from the point with coordinates the minimum values of P_1 and P_2, which is considered as a Utopian point P_i^U for $i = 1, 2$ (where i represents the two axis [22]). More specifically, the coordinates of the Utopian point in each plot are the minimum values of each objective. Furthermore, each objective solution is normalised according to:

$$P_i^{norm} = \frac{P_i(\beta) - P_i^U}{P_i^{max} - P_i^U} \tag{21}$$

In order to demonstrate the behaviour of the optimisation problem, extreme cases of weights γ_1 and γ_2 are used demonstrating the impact of preference towards one of the two objective functions. The same network and control simulation parameters are used as in the previous section, as variability of network conditions is not examined.

The first set of plots in Figure 5(a) depicts the use of scaling parameters $\gamma_1 = 0.1$ and $\gamma_2 = 0.9$. This means that the master problem objective function should act in favour of the P_2 problem. On the other hand, in Figure 5(b) the master objective function acts in favour of the P_1 problem as the scaling parameters are $\gamma_1 = 0.2$ and $\gamma_2 = 0.1$. Indeed it can be observed that for all scenarios of Figure 5(a) the value of β is significantly lower than in 5(b), with the exception of Scenario 4 (free space movement) which is slightly lower. The latter is due to the very small change of objective $P1$ values, i.e., the CPLF of PCP doesn't change a lot for the corresponding values of d_H.

Another important thing to pay attention to is the behaviour of the optimisation of β depending on the scenario. Due to the higher delay requirements of Scenarios 1, 2 and 3 the it is evident that the change in the value of β between the two different scaling parameter configurations is significant. The opposite can be said for Scenario 4 which has lower delay requirements due to the absence of contact.

VII. CONCLUSION

In this paper, we formulate a generic model for control performance of haptic communications, as a polynomial function, and demonstrate how this performance is affected by a network scheduling discipline based on priority queues with priority jumps. The chosen dynamic priority scheduling discipline assumes high and low priority critical traffic and offers great flexibility in terms of improving waiting time of low priority traffic to avoid overprovision of high priority queue. Nevertheless, this has an impact on efficiency in utilisation of communication resources which affects waiting time of high priority packets of a flow with haptic communication requirements.

For this reason, we formulate an optimisation problem that maximises performance of bilateral teleoperation and allows comparison among different bilateral teleoperation control schemes, while minimising the waiting time of the low priority queue. Packet waiting times are calculated based on the analysis of the HOL-MBP discipline. Through a numerical study, we demonstrate both control and communication performance considering haptic communication scenarios.

Finally, the proposed control performance model is agnostic to the possible networking components that may affect the end-to-end communication latency (e.g. a queuing discipline) and therefore the use of the control performance model can be expanded to components that can operate under different conditions.

APPENDIX

Acronym	Definition
AMFC	Adaptive Motion/Force Control
CPLF	Control Performance Loss Function
C-RAN	Cloud-Radio Access Network
FR	Force Reflection
HOL-MBP	Head-of-Line Merge-by-Probability
HOL-PJ	Head-of-Line Priority Jump
IS	Intrinsically Stable
MEC	Multi-access Edge Computing
PC	Predictive Control
PCP	Predictive control with Passivity
PE	Position Error
PGF	Probability Generating Functions
PP	Probability Priority
PS	Possibly Stable
QoE	Quality of Experience
QoS	Quality of Service
SP	Strict Priority
TCP	Transport Control Protocol
URLLC	Ultra-reliable Low-latency Communication
VNF	Virtual Network Function

Symbol	Definition
A_T	PGF of total number of arrivals
β	jump probability for HOL-MBP
B_m	Viscous coefficient of primary manipulator
B_i	Communication network impedance (used in PCP)
B_p	Perceived damping
d	delay
Δ	Drift error
δ	Tracking error
$E[d]$	Mean value of delay of any arbitrary packet
$E[d_H]$	Mean value of delay in high priority queue
$E[d_L]$	Mean value of delay in low priority queue
$E[p_T]$	Total number of packets in the system
F_e	Environment force
F_h	Human force
F_m	Output force of primary manipulator
F_{pc}	Primary manipulator controller force
F_s	Output force of secondary man ipulator
F_{sc}	Secondary manipulator controller force
K_c	Controller gain parameter
K_e	Environment stiffness
K_p	Perceived environment stiffness
λ	Lagrange multiplier
λ_T	Total arrival rate
λ_{TT}	Second partial derivative of arrival process PGF
λ_1	Arrival rate of high priority traffic
λ_2	Arrival rate of low priority traffic
v_m	Primary manipulator velocity
v_s	Secondary manipulator velocity
Y	recursive function (numerically computed)
ϕ_l	normalization weights

REFERENCES

[1] M. Dohler, T. Mahmoodi, M. A. Lema, M. Condoluci, F. Sardis, K. Antonakoglou, and H. Aghvami, "Internet of skills, where robotics meets AI, 5G and the tactile Internet," in *Proc. Eur. Conf. Netw. Commun. (EuCNC)*, Jun. 2017, pp. 1–5.

[2] K. Antonakoglou, X. Xu, E. Steinbach, T. Mahmoodi, and M. Dohler, "Toward haptic communications over the 5G tactile Internet," *IEEE Commun. Surveys Tuts.*, vol. 20, no. 4, pp. 3034–3059, 4th Quart., 2018.

[3] P. F. Hokayem and M. W. Spong, "Bilateral teleoperation: An historical survey," *Automatica*, vol. 42, no. 12, pp. 2035–2057, Dec. 2006.

[4] T. Maertens, J. Walraevens, and H. Bruneel, "On priority queues with priority jumps," *Perform. Eval.*, vol. 63, no. 12, pp. 1235–1252, Dec. 2006.

[5] X. Wei, Q. Duan, and L. Zhou, "A QoE-driven tactile Internet architecture for smart city," *IEEE Netw.*, vol. 34, no. 1, pp. 130–136, Jan. 2020.

[6] M. Aazam, K. A. Harras, and S. Zeadally, "Fog computing for 5G tactile industrial Internet of Things: QoE-aware resource allocation model," *IEEE Trans. Ind. Informat.*, vol. 15, no. 5, pp. 3085–3092, May 2019.

[7] X. Ge, R. Zhou, and Q. Li, "5G NFV-based tactile Internet for mission-critical IoT services," *IEEE Internet Things J.*, vol. 7, no. 7, pp. 6150–6163, Jul. 2020.

[8] X. Xu, Q. Liu, and E. Steinbach, "Toward QoE-driven dynamic control scheme switching for time-delayed teleoperation systems: A dedicated case study," in *Proc. IEEE Int. Symp. Haptic, Audio Vis. Environ. Games (HAVE)*, Oct. 2017, pp. 1–6.

[9] M. Condoluci, T. Mahmoodi, E. Steinbach, and M. Dohler, "Soft resource reservation for low-delayed teleoperation over mobile networks," *IEEE Access*, vol. 5, pp. 10445–10455, 2017.

[10] S. Liu, M. Li, X. Xu, E. Steinbach, and Q. Liu, "QoE-driven uplink scheduling for haptic communications over 5G enabled tactile Internet," in *Proc. IEEE Int. Symp. Haptic, Audio Vis. Environ. Games (HAVE)*, Sep. 2018, pp. 1–5.

[11] A. E. Kalor, R. Guillaume, J. J. Nielsen, A. Mueller, and P. Popovski, "Network slicing in industry 4.0 applications: Abstraction methods and end-to-end analysis," *IEEE Trans. Ind. Informat.*, vol. 14, no. 12, pp. 5419–5427, Dec. 2018.

[12] A. Nasrallah, A. S. Thyagaturu, Z. Alharbi, C. Wang, X. Shao, M. Reisslein, and H. ElBakoury, "Ultra-low latency (ULL) networks: The IEEE TSN and IETF DetNet standards and related 5G ULL research," *IEEE Commun. Surveys Tuts.*, vol. 21, no. 1, pp. 88–145, 1st Quart., 2019.
[13] J. Chen, "Corrections to 'On computing the maximal delay intervals for stability of linear delay systems,'" *IEEE Trans. Autom. Control*, vol. 45, no. 11, p. 2198, Nov. 2000.
[14] P. Arcara and C. Melchiorri, "Control schemes for teleoperation with time delay: A comparative study," *Robot. Auton. Syst.*, vol. 38, no. 1, pp. 49–64, 2002.
[15] D. A. Lawrence, "Stability and transparency in bilateral teleoperation," *IEEE Trans. Robot. Autom.*, vol. 9, no. 5, pp. 624–637, Oct. 1993.
[16] B. Davie, A. Charny, J. Bennet, K. Benson, J. L. Boudec, W. Courtney, S. Davari, V. Firoiu, and D. Stiliadis, *An Expedited Forwarding PHB (Per-Hop Behavior)*, document RFC 3246, Mar. 2002.
[17] J. J. Bae and T. Suda, "Survey of traffic control schemes and protocols in ATM networks," *Proc. IEEE*, vol. 79, no. 2, pp. 170–189, Feb. 1991.
[18] Y. Oh, C. Kim, and A. Melikov, "A space merging approach to the analysis of the performance of queueing models with finite buffers and priority jumps," *Ind. Eng. Manage. Syst.*, vol. 12, no. 3, pp. 274–280, Sep. 2013.
[19] Y. Jiang, C.-K. Tham, and C.-C. Ko, "Delay analysis of a probabilistic priority discipline," *Eur. Trans. Telecommun.*, vol. 13, no. 6, pp. 563–577, Nov. 2002.
[20] *System Architecture for the 5G System*, document 23.501 Rel 16, 3GPP, Sep. 2020.
[21] I. Y. Kim and O. L. de Weck, "Adaptive weighted-sum method for bi-objective optimization: Pareto front generation," *Struct. Multidisciplinary Optim.*, vol. 29, no. 2, pp. 149–158, Feb. 2005.
[22] J. Arora, *Introduction to Optimum Design*. Amsterdam, The Netherlands: Elsevier, 2004.

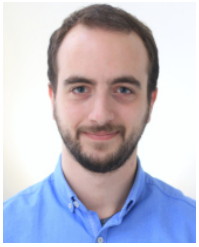

KONSTANTINOS ANTONAKOGLOU (Member, IEEE) received the M.Sc. degree in control and computing from the National and Kapodistrian University of Athens, in 2014, and the Ph.D. degree in telecommunications from King's College London, in 2020. He is currently a Research Associate with King's College London involved in the EU-Korea collaboration project PriMO-5G and the EPSRC-funded project INITIATE. His research interests include haptic communication systems over networks, mobile cloud computing, and edge-assisted AI systems.

MALIHEH MAHLOUJI received the master's degree in telecommunication systems from the Sharif University of Technology, Tehran, Iran. She is currently working in the telecom industry as a Data Scientist, analyzing mobile data with focus on network performance. She was previously a Research Assistant with the Centre for Telecommunications Research, King's College London, for a period of two years, working on the H2020 5GCAR project.

TOKTAM MAHMOODI (Senior Member, IEEE) received the B.Sc. degree in electrical engineering from the Sharif University of Technology, Iran, and the Ph.D. degree in telecommunications from King's College London, U.K. She was a Visiting Research Scientist with F5 Networks, San Jose, CA, USA, in 2013, a Postdoctoral Research Associate with the ISN Research Group, Electrical and Electronic Engineering Department, Imperial College, from 2010 to 2011, and a Mobile VCE Researcher, from 2006 to 2009. She has also worked in mobile and personal communications industry, from 2002 to 2006. She has worked with a Research and Development Team on developing DECT standard for WLL applications. She is currently the Head of the Centre for Telecommunications Research, Department of Informatics, King's College London. She has contributed to, and led a number of FP7, H2020, and EPSRC funded projects, advancing mobile and wireless communication networks. Her research interests include 5G communications, network virtualization, and low latency networking.